Korean J. Crystallography
Vol. 11, No. 4, pp.195~199, 2000

Microstructural Characterization of $CaTiO_3$-$NdAlO_3$-Based Ceramics

Danilo Suvorov, Goran Drazic, Matjaz Valant and Bostjan Jancar

"Jozef Stefan" Institute, Ceramics Department, Jamova 39, SI-1001 Ljubljana, Slovenia

Abstract

Ceramics based on $CaTiO_3$-$NdAlO_3$ solid solutions were synthesized in order to study their dielectric microwave properties. Microstructural analysis was performed with scanning electron microscopy (SEM) and transmission electron microscopy (TEM) using different analytical methods such as energy-dispersive X-ray spectroscopy (EDXS). It was observed that the heating conditions during sintering and cooling strongly affect the microstructural development of $CaTiO_3$-$NdAlO_3$-based ceramics. Various types and concentrations of structural defects were identified, for example, dislocations, twins and/or antiphase boundaries. All such defects resulted in a degradation of the dielectric microwave properties, in particular the quality factor Q. Dielectric properties of $CaTiO_3$-$NdAlO_3$-based ceramics can be improved by an appropriate thermal treatment of ceramics which results in a decrease in the concentration of the identified microstructural defects.

1. Introduction

Microwave dielectric ceramics for wireless and global communications must exhibit low dielectric losses (high Q-values), high relative permittivities (ε'_r) and temperature stable dielectric properties. There is a constant demand for electronic devices with improved properties that will enable further miniaturization and increase the reliability of microwave components. Today's materials with $\varepsilon'_r < 35$ and Qxf_r ~50.000 need to be replaced by materials with higher relative permittivity values ($\varepsilon'_r > 45$) which maintain high quality factors (Qxf_r~45.000). It has already been demonstrated that ceramics based on $La_{2/3}TiO_3$-$LaAlO_3$ solid solutions can fulfill some of these demands.[1)]

Another promising example are ceramics based on $CaTiO_3$-$NdAlO_3$ solid solutions.[2,3)] $CaTiO_3$ is an orthorhombic perovskite with ε'_r~170, Qxf_r~3.500 and a high positive temperature coefficient of resonant frequency τ_f ($\tau_f = +800$ ppm/K).[4,5)] At 1300°C it undergoes a high-temperature phase transition to form a cubic structure. $NdAlO_3$ is a rhombohedral perovskite with ε'_r~22, Qxf_r~58.000 and a negative temperature coefficient of resonant frequency ($\tau_f = -33$ ppm/K).[6)] Therefore, depending on the chemical composition of the $CaTiO_3$-$NdAlO_3$ solid solution, relative permittivities (ε'_r) higher than 45 can be obtained with high quality factors ($Qxf_r > 40.000$) and a temperature-stable coefficient of resonant frequency τ_f. However, the resulting dielectric microwave properties depend strongly on the firing conditions, especially on the sintering temperature and the cooling rate, indicating the possibility that the structural development during sintering and cooling plays a key role.

In the present work, preliminary results of the microstructural characterization of 70 mol. % $CaTiO_3$-30 mol. % $NdAlO_3$-based ceramics using a SEM and TEM-EDXS analysis are reported.

2. Experimental

Samples were synthesized by a solid-state-reaction method. Starting powders of $CaCO_3$ (Johnson Matthey 99,99%), TiO_2 (Johnson Matthey > 99%), Nd_2O_3 (Johnson Matthey 99,99%) and Al_2O_3 (Johnson Matthey 99,99%) were mixed in alcohol, dried, pressed into pellets and calcined with intermediate crushing for 40 hours in the temperature range between 1350°C and 1450°C until equilibrium was achieved. For the purpose of microwave-prop-

erty measurements and microstructural analysis, calcined powders were isostatically pressed into discs and sintered at temperatures between 1350°C and 1500°C for 10 hours.

The progress of the reaction was monitored by X-ray diffraction analyses (XRD) with a Philips PW 1710 X-ray powder diffractometer using CuK_α radiation. Microstructural analysis of the samples was performed with a JEOL JXA-840A scanning electron microscope (SEM) equipped with a Tracor-Northern energy-dispersive X-ray spectrometer (EDXS) and with a JEOL 2000FX transmission electron microscope (TEM) with attached Link AN 10000 EDXS system.

3. Results and Discussion

The typical microstructure of a ceramic with a composition 70 mol. % $CaTiO_3$ 30 mol. % $NdAlO_3$ after sintering at 1450°C for 10 hours is shown in Fig. 1. Using energy-dispersive X-ray spectroscopy (EDXS) it was found that just one phase was present in the samples. The microstructure is dense, with average grain size of approximately 10 μm. Most of the remaining porosity is closed porosity.

In Fig. 2 a TEM micrograph of an area near the grain boundary (GB) in a $CaTiO_3$-$NdAlO_3$ sample is shown. The grains are composed of many smaller, irregularly shaped domains (D). Beside domains, planar loop-forming features were observed inside the grains (Fig. 3a and 3b). Due to their characteristic shape, and based on bright-field (BF)-dark-field (CDF) experiments (two beam case condition),

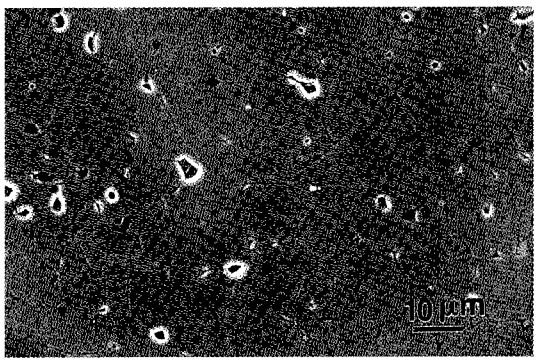

Fig. 1. Microstructure of 70 mol. % $CaTiO_3$ 30 mol. % $NdAlO_3$ based ceramics after sintering at 1450°C for 10 hours (cooling rate 5°C/minute).

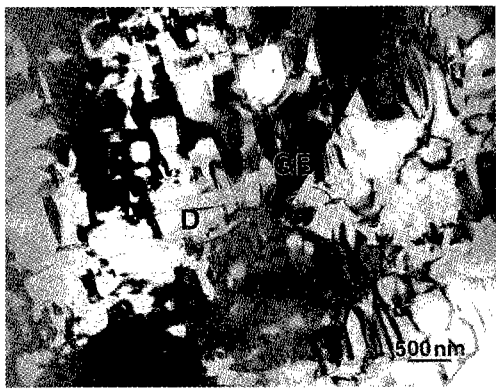

Fig. 2. TEM mircographs of a $CaTiO_3$-$NdAlO_3$ sample: area near the grain boundary (GB) showing the presence of domains (D).

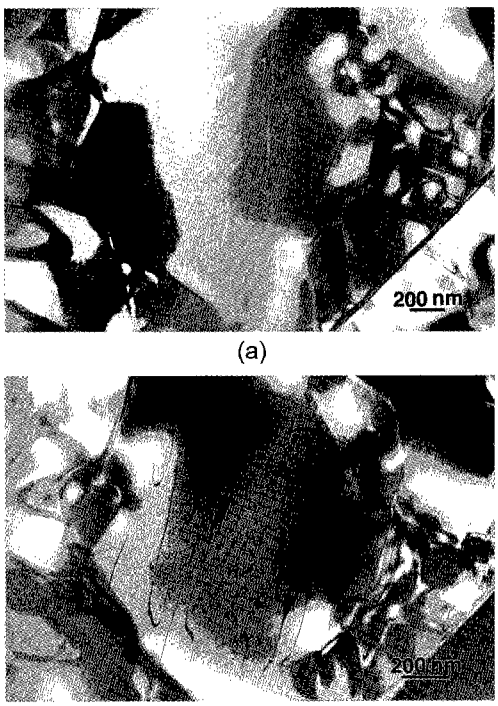

Fig. 3. TEM micrographs of antiphase boundaries in a $CaTiO_3$-$NdAlO_3$ sample: a) bright field, b) dark field. Note symmetrical contrast in BF and inversely symmetrical contrast of fringes in CDF, characteristic of APB boundaries.

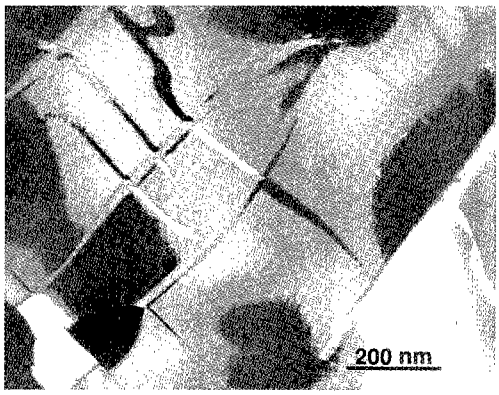

Fig. 4. TEM micrograph (CDF) of part of a grain where two types of planar defects (domain boundaries and APB) are clearly seen.

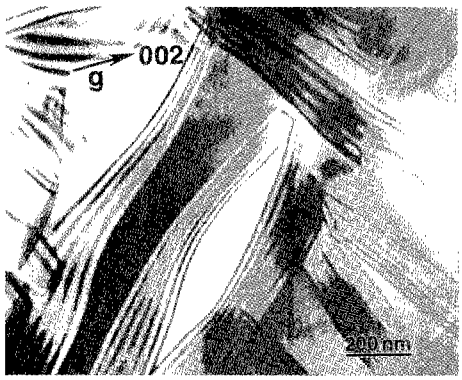

(a)

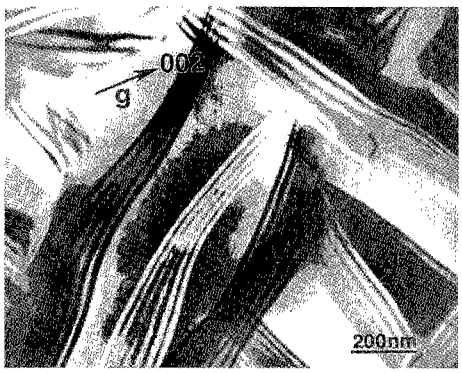

(b)

Fig. 5. TEM micrographs of tilted domain boundaries in a $CaTiO_3$-$NdAlO_3$ sample: a) bright field, b) dark field. Note asymmetrical contrast in BF and symmetrical contrast of fringes in CDF, characteristic for d-boundaries.

and the contrast and symmetry of the fringes, we determined that these planar defects (boundaries) are of the π-type, so we were able to conclude that they are antiphase boundaries (APB).

In Fig. 4 (dark-field micrograph) a part of a grain with two types of planar defects, i.e. domain boundaries and APBs, is presented. It is clear that antiphase boundaries are passing unimpeded through the domain boundaries. The change in contrast of APBs when passing through adjacent domains is clearly visible and indicates the different crystallographic orientation of the domains.

The domains are separated by boundaries which where found to be of δ-type, typical for twins and ferroelectric domains. In Fig. 5, bright-field and dark-field TEM micrographs of tilted domain boundaries are shown (two beam case condition). The asymmetrical contrast of fringes in bright field and the symmetrical contrast in dark field clearly confirm the presence of d-boundaries.

In Fig. 6 a TEM micrograph of a region with domains inside a grain is shown. From this region an electron diffraction pattern was recorded (Fig. 7).

The SAED pattern shown in Fig. 6 exhibits cubic symmetry and gives pseudospacings of around 0.76 nm. In $CaTiO_3$ doped with Pb, different types of ordering[7,8] such as chemical ordering and ordering due to tilting of the octahedra[9] were found. The

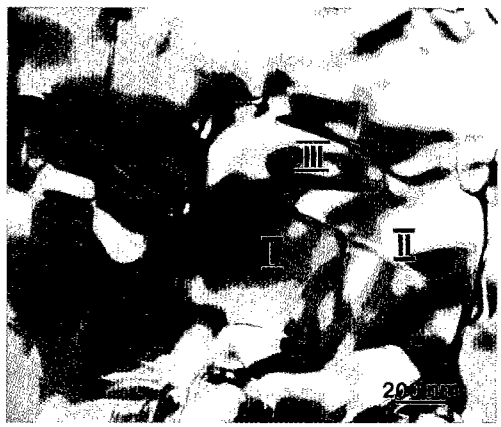

Fig. 6. TEM mircograph of a $CaTiO_3$-$NdAlO_3$ sample: domains inside a grain with labeled areas (I, II, III) where SAED pattern shown in Fig. 7 was recorded.

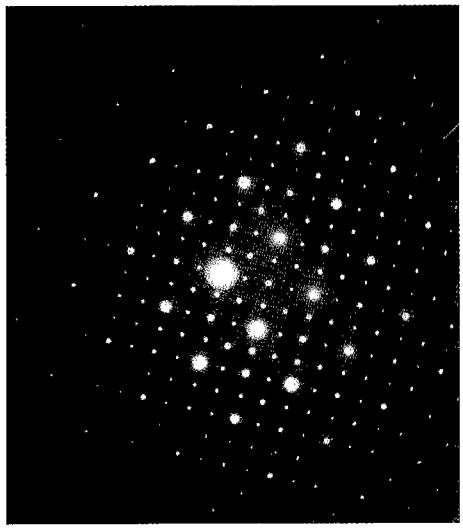

Fig. 7. Selected area electron diffraction (SAED) pattern from a region shown in Fig. 6.

unit cell was cubic with a = 0.38 nm and various superstructure reflections were observed in the [001] zone (at {h/2 0 0}, {h/2 k/2 0} and {h/2 k/2 l/2} positions). In the case of the surperstructure, the cell was doubled with a = 0.76 nm. In some other compositions of $(Pb,Ca)TiO_3$[10] a tetragonal unit cell with a = 0.54 nm and c = 0.76 nm was found and was explained by the chemical ordering of A-site atoms.

Using a smaller aperture size and SAED patterns from three adjacent domains (labeled as I, II and III in Fig. 5), it was noticed that each domain has its own diffraction pattern. Schematic drawings of this patterns, indexed for an orthorhombic (a = 0.5409 nm, b = 0.7678 nm, c =0.5455 nm) unit cell are displayed in Fig. 8. From the zone axis the crystallographic relations between adjacent domains were obtained. It was found that {101} planes in one domain are parallel to {010} planes of the second and {101} planes of the third domain. {121} planes are parallel to {121} planes in the second and to {100} planes in the third domains. A pair of domains, oriented in <101> directions, is rotated by 90° to each other. These results indicate the presence of rotational twins in the $CaTiO_3$-$NdAlO_3$ material.

The twining of pure $CaTiO_3$ was studied using high-resolution electron microscopy by White *et al.*[11] They found that twinning results in domains related to each other by either a 180° or a 90° rotation about an axis perpendicular to the {101} planes. Twin boundaries were found to be complex and consisted of intergrowths of the various composition planes, such as {101}, {010} and {121}.

The reasons for the heavily twinned structure in $CaTiO_3$-$NdAlO_3$ ceramics and the structure of the twin and antiphase boundaries will be investigated in more detail in the future.

4. Conclusions

Ceramics based on $CaTiO_3$-$NdAlO_3$ solid solu-

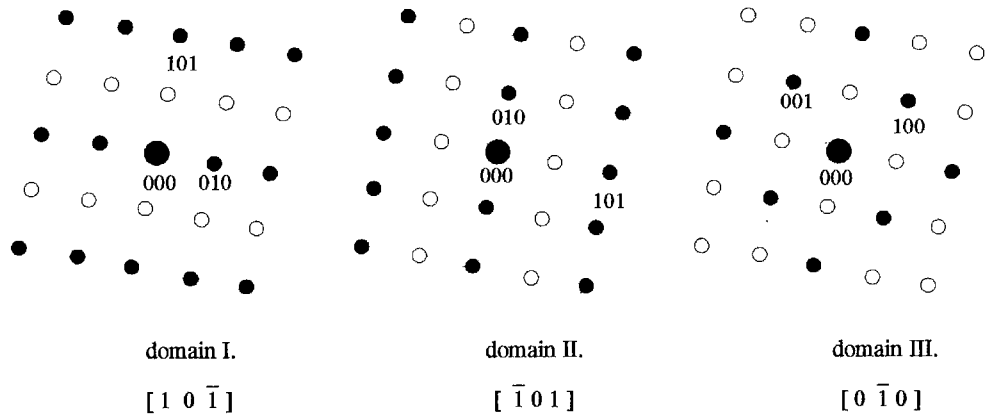

Fig. 8. Schematic drawings of diffraction patterns obtained from different domains, indexed as a rhombohedral phase. (Open circles represent missing reflections.)

tions show very promising dielectric microwave properties: ε'_r higher than 45, $Qxf_r > 40.000$ and a temperature-stable coefficient of resonant frequency t_f. Microstructural analysis confirmed the presence of various types of defects in these ceramics which strongly influence the resulting microwave properties. Depending on sintering temperature and cooling rate, dislocations, twins and antiphase boundaries were found. The concentration of the defects is high which leads us to the conclusion that the resulting dielectric microwave properties of such ceramics can be even further improved by proper thermal treatment resulting in a decrease of the concentration of the identified microstructural defects.

References

1) Suvorov, D., Šapin, S., Valant, M. and Kolar, D., *J. Mater. Sci.*, **33**(1), 85-89, (1998).
2) Suvorov, D. and Valant, M., 101st Ann. Meet. AcerS, Indianapolis, May 1999, Book of Abstracts (1999).
3) Jancar, B., Suvorov, D. and Valant, M. Submitted for publication in *J. Mater. Sci. Lett.* (2000).
4) Kell, R. C., Greenham, A. C. and Olds, G. C. E., *J. Am. Ceram. Soc.*, **56**(7), 352 (1973).
5) Kucheiko, S., Choi, J. W., Kim, H. J. and Jung, H. J., *J. Am. Ceram. Soc.*, **79**(10), 2739 (1996).
6) Cho, S. Y., Kim, I. T. and Hong, K. S., *J. Mater. Res.*, **14**(1), 114 (1999).
7) King, G. and Goo, E. K., *J. Am. Ceram. Soc.*, Vol. **73**[6], 1534 (1990).
8) Ganesh, R. and Goo, E. K., *J. Am. Ceram. Soc.*, Vol. **80**[3], 653 (1997).
9) Reaney, I. M., Colla, E. L. and Setter, N., *Jpn. J. Appl. Phys.*, Vol. **33**, 3984 (1994).
10) King, G., Goo, E., Yamamoto, T. and Okazaki, K., *J. Am. Ceram. Soc.*, Vol. **71**[6], 454 (1988).
11) White, T. J., Segall, R. L., Barry, J. E. and Hutchinsone, J. L., *Acta Cryst.*, **B41**, 93 (1985).